Assessing epithelial cell nuclear morphology by using azimuthal light scattering spectroscopy

Chung-Chieh Yu, Condon Lau, James W. Tunnell,* Martin Hunter, Maxim Kalashnikov, and Christopher Fang-Yen

G. R. Harrison Spectroscopy Laboratory, Massachusetts Institute of Technology, Cambridge, Massachusetts 02139

Stephen F. Fulghum

Newton Laboratories, Inc., Woburn, Massachusetts 01801

Kamran Badizadegan,† Ramachandra R. Dasari, and Michael S. Feld

G. R. Harrison Spectroscopy Laboratory, Massachusetts Institute of Technology, Cambridge, Massachusetts 02139

Received June 30, 2006; accepted July 21, 2006;
posted August 10, 2006 (Doc. ID 72519); published October 11, 2006

We describe azimuthal light scattering spectroscopy (ϕ/LSS), a novel technique for assessing epithelial-cell nuclear morphology. The difference between the spectra measured at azimuthal angles $\phi=0°$ and $\phi=90°$ preferentially isolates the single backscattering contribution due to large ($\sim 10\ \mu$m) structures such as epithelial cell nuclei by discriminating against scattering from smaller organelles and diffusive background. We demonstrate the feasibility of using ϕ/LSS for cancer detection by showing that spectra from cancerous colon tissue exhibit significantly greater azimuthal asymmetry than spectra from normal colonic tissues.

OCIS codes: 290.0290, 170.6510, 170.4580, 170.3890.

Light scattering spectroscopy (LSS) is an optical technique in which quantitative information of cell organelle morphology is extracted via measurement of the spectrum and/or angular dependence of backscattered light.[1–7] Although much work has been focused on the light scattering properties of mitochondria,[1–4] we and others have described the principles and potential clinical applications of light scattering from epithelial cell nuclei.[5–7] The use of LSS to measure epithelial cell nuclear size distribution *in situ* is of particular interest because enlarged and crowded nuclei are early indicators of cancer development. This nuclear-based approach relies on isolating the single backscattering signal associated with nuclei from the diffusive background signal and the single backscattering from smaller organelles. Our group previously addressed this task by modeling the general spectral features of the diffusive background.[5] Subsequently, we[6] and Sokolov *et al.*[7] proposed using polarized light scattering spectroscopy (p/LSS) to experimentally isolate single backscattering from other contributions. The primary focus of LSS research has been removing the diffuse reflectance, and surprisingly little attention has been focused on removing the single backscattering contribution from smaller organelles such as mitochondria (diameter $d \leq 3\ \mu$m), even though this contribution may be substantial.[8] Here, we show that rejection of small organelle scattering can be performed by taking advantage of the asymmetry with respect to azimuthal angle (measured relative to incident polarization direction) in single scattering spectra from large particles. Additionally, we demonstrate the clinical potential of this method to assess epithelial cell nuclear morphology *in situ*.

A randomly oriented distribution of nuclei and mitochondria embedded in tissue can be modeled as a collection of spherical Mie scatterers with refractive indices higher than that of the surrounding cytoplasm and characteristic diameters $d > 5\ \mu$m and $d \sim 1$ to $2\ \mu$m, respectively.[1–7] The scattered intensity from a sphere illuminated by polarized light is a function of d, scattering polar angle θ (between the incident and scattered light directions), azimuthal angle ϕ (between the incident light polarization and scattering plane), wavelength λ, and particle refractive index m relative to the surrounding medium.[9] For singly backscattered light ($\theta \sim 180°$) with polarization the same as the incident light, we plot the calculated angular scattering intensity maps of scatterers with d of 10, 5, and 2 μm (Fig. 1). Note that for 10 μm particles the scattering exhibits azimuthal asymmetry at $\theta \sim 178°$, whereas for 2 μm particles, scattering is virtually ϕ-independent at the same θ.

We define the ϕ/LSS spectrum, $I_{\Delta\phi}(\lambda) = R_{\phi=0°}(\lambda) - R_{\phi=90°}(\lambda)$, as the difference between tissue reflectance spectra $R_{\phi=0°}(\lambda)$ and $R_{\phi=90°}(\lambda)$ measured with the same polarization at solid angles $\Omega_{\phi=0°}$ and $\Omega_{\phi=90°}$, which are centered at the same θ close to 180°

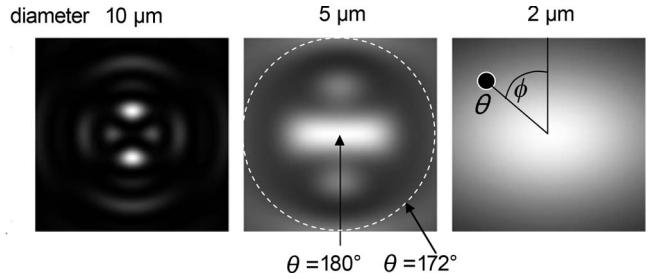

Fig. 1. Scattering intensity angular maps (radial direction, θ, angular direction, ϕ) for $\theta = 180°$ (center of plot) to 172° and $\phi = 0°$ to 360°, computed from Mie theory with $m = 1.059$ and $\lambda = 450$ nm.

0146-9592/06/213119-3/$15.00

but at azimuthal angles $\phi=0°$ and $\phi=90°$, respectively. Since diffusive background is ϕ independent and small particle single backscattering exhibits little ϕ asymmetry (Fig. 1), $I_{\Delta\phi}(\lambda)$ can be used to extract the single backscattering contribution specifically from epithelial cell nuclei.

A schematic diagram of the experimental setup is shown in Fig. 2. A beam from a xenon arc lamp (Oriel, Inc.) is color filtered (FWHM = 10 nm) by a monochromator (Oriel, Inc.) and collimated by lens L1. The 4 mm diameter opening of the mask is imaged 1:1 onto the sample by a 4*f* system (L2 and L3). Iris 1 restricts the divergence of the light to a half-angle of 0.5°. Reflectance from the sample is redirected by a beam splitter and imaged via a 4*f* system (L4 and L5) onto Iris 2, which selects the detection area to match the illuminated area. Polarizers P1 and P2 ensure that the polarizations of the collected and incident light are parallel. The CCD (Photometrics CoolSNAP HQ) is positioned at the focal plane of L6. As a result, reflectance from the sample at different angles is collected by different pixels of the CCD. Sample reflectance is recorded at each incident wavelength, which is stepped from 450 to 700 nm in 5 nm increments. The recorded reflectance angular maps are processed to yield two reflectance spectra, $R_{\phi=0°}(\lambda)$ and $R_{\phi=90°}(\lambda)$, for $\phi=0°\pm5°$ and $90°\pm5°$, respectively. The polar angle $\theta=\theta_0\pm0.5°$ for both spectra.

We conducted tissue phantom measurements to test the effectiveness of ϕ/LSS for detecting azimuthal asymmetry of single backscattering from nuclear-size particles in the presence of diffusive background, absorption, and mitochondria-size particle single scattering. Our tissue phantoms consist of two layers separated by a thin window. The top layer, which simulates the epithelium, is a mixture of 10 μm (Duke Scientific) and 1 μm (Polysciences) diameter spheres, representing nuclei and mitochondria, respectively, suspended in a water–glycerol mixture. The bottom layer, which simulates the underlying connective tissue, consists of Intralipid containing 5 mg/mL hemoglobin to provide physiologically relevant diffusive background and absorption. We measured reflectance spectra $R_{\phi=0°}(\lambda)$ [Fig. 3(a)] and $R_{\phi=90°}(\lambda)$ at $\theta_0=177.5°$, with the ratio between the number of 1 and 10 μm spheres (see legend) varied to span the range of ratios between the number of mitochondria and nuclei in human cells.

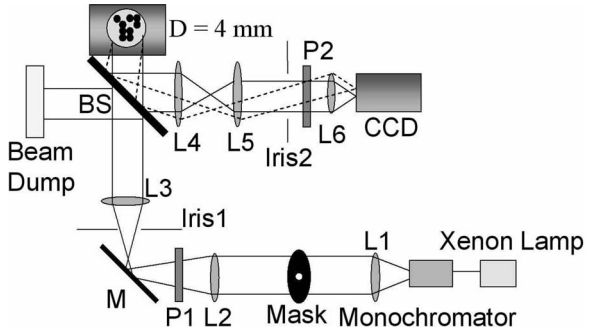

Fig. 2. ϕ/LSS experimental system. BS, beam splitter; M, mirror. Other abbreviations defined in text.

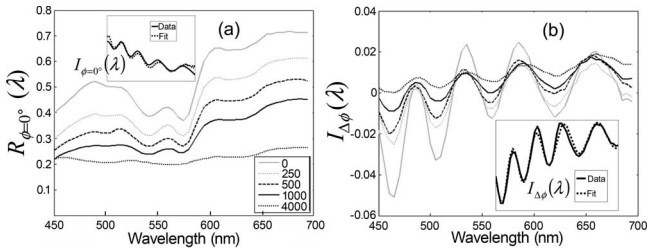

Fig. 3. (a) Reflectance $R_{\phi=0°}(\lambda)$ and (b) intensity $I_{\Delta\phi}(\lambda)$ for phantoms with varying numbers of 1 μm spheres measured at $\theta=177.5°$. The legend shows the ratio between number of 1 μm spheres and 10 μm spheres. The optical density of 10 μm spheres is approximately 0.2. The insets of (a) and (b) show $I_{\phi=0°}(\lambda)$ and $I_{\Delta\phi}(\lambda)$ measured from 10 μm spheres alone (no small spheres, no diffuse background) and corresponding fits based on Mie theory.

These measured results in Fig. 3(a) demonstrate that the signal contributed from other scatterers and absorbers significantly masks the single backscattering intensity spectrum from the 10 μm spheres [$I_{\phi=0°}(\lambda)$, inset of Fig. 3(a)], which was independently measured from 10 μm diameter spheres alone without diffusive background or smaller spheres. We then take the difference between $R_{\phi=0°}(\lambda)$ and $R_{\phi=90°}(\lambda)$ to obtain $I_{\Delta\phi}(\lambda)$ [Fig. 3(b)]. We compare $I_{\Delta\phi}(\lambda)$ measured from 10 μm spheres in the presence of other scatterers and absorbers with $I_{\Delta\phi}(\lambda)$ measured from 10 μm spheres alone [inset of Fig. 3(b)]. The results show that the oscillatory features are preserved for all conditions tested. We note that the contrast of the oscillatory component decreases as the density of 1 μm spheres is increased. This occurs because the 1 μm spheres partially decollimate and depolarize the light incident on the 10 μm spheres. Thus the single backscattering azimuthal asymmetry from 10 μm spheres is reduced. However, this should not affect the effectiveness of extracting the size distribution and refractive index of the spheres from ϕ/LSS, since the oscillatory component on which the extraction is based is preserved. To quantify the accuracy of ϕ/LSS, we fit the spectra of Fig. 3(b) to Mie theory predictions. We assume the sizes of scatterers are distributed with a normal probability density function with mean diameter d and standard deviation σ. We also assume that the scattering is from N independent scatterers, i.e., $I_{\Delta\phi}^{\text{fit}}(\lambda)=NI_{\Delta\phi}(d,\sigma,m)$. We search at different values of d, σ, m, and N, $\theta_0=177.5°$, to find the combination that minimizes the least-squares error between the data and the fit. All extracted values of d agreed with the manufacturer's specifications to within 6%.

We conducted ϕ/LSS studies in *ex vivo* samples of colonic mucosa to measure epithelial nuclear size. Normal and neoplastic colon tissues were obtained from excess/discarded materials removed at surgery for clinical indications. Tissue reflectance spectra were collected at room temperature. After each experiment, samples were fixed in 10% neutral buffered formalin and embedded in paraffin; 5 μm sections were cut and stained with hematoxylin and eosin for expert pathological diagnosis and nuclear morphom-

etry. Pathological diagnoses were recorded and independently confirmed by K. Badizadegan. For nuclear morphometry on histological sections, at least 100 surface epithelial nuclei (including intraepithelial lymphocytes) were selected from five randomly selected photographed fields. Epithelial nuclei with a well-defined nuclear contour in the plane of sections were selected using Photoshop (Adobe Systems) and Fovea Pro 3.0 (Reindeer Graphics) segmentation tools. A binary image of the segmented nuclei was constructed and used for feature analysis. Given that epithelial cells often have an elongated nucleus, the data presented here represent the average equivalent diameter, d_M, defined as the diameter of a circle with the same cross-sectional area as the measured nucleus.

The ϕ/LSS spectrum, $I_{\Delta\phi}(\lambda)$, was measured from four cancerous colonic mucosa from four cancer patients and eight normal colonic mucosa from the four cancer patients and three additional cancer-free patients. Figure 4(a) shows one normal and one cancerous spectrum, along with their Mie theory fits. The azimuthal asymmetry was found to be more pronounced in the cancerous tissue. The spectra were compared with Mie theory predictions to extract the characteristic nuclear morphology parameters m, σ, N, and d_{LSS}, which is compared with d_M in Fig. 4(b).

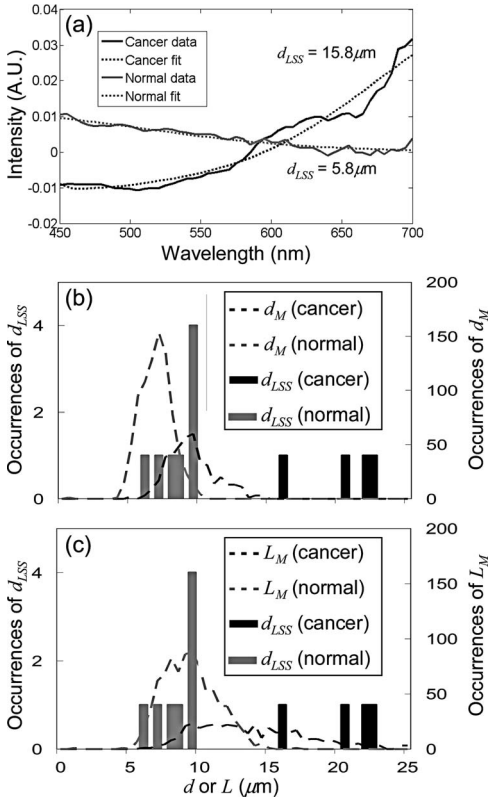

Fig. 4. (a) $I_{\Delta\phi}(\lambda)$ measured at $\theta_0 = 177.5°$ from two colon tissue samples. (b) Histograms of d_{LSS} and d_M (defined in text). (c) Histograms of d_{LSS} and L_M (defined in text). The y axes indicate the number of occurrences. For morphometry results, the measured d_M and L_M from all samples are binned in 0.5 μm units. For ϕ/LSS results, the 12 extracted d_{LSS} are binned in 0.5 μm units.

For normal tissue, d_{LSS} is consistent with d_M. However, all the d_{LSS} for cancerous tissue lie outside the d_M size distribution. We note that this deviation is consistent with the fact that cancerous epithelial cell nuclei are more elongated. Therefore, we consider the nonspherical shape of each nucleus by fitting the nuclear shape observed under the microscope to a rectangle and extracting its length (L_M) and width. We find that d_{LSS} is still consistent with L_M for normal tissue [see Fig. 4(c)]. Furthermore, all cancerous d_{LSS} are inside the L_M size distribution. These findings suggest that d_{LSS} is consistent with the longest dimension of the nonspherical nucleus.

This study is to our knowledge the first demonstration of the use of scattering azimuthal asymmetry to extract nuclear morphological parameters in cancerous and normal colon tissues. The characteristic size d_{LSS} separates cancer from normal tissue and appears to increase with length and volume of the epithelial cell nuclei. Future work will explore the diagnostic abilities of azimuthal asymmetry in precancerous tissue and different organ types using ϕ/LSS both in a wide-area imaging system and in a point-probe geometry. These developments will advance the use of optical spectroscopy for providing accurate, real-time, and minimally invasive cancer diagnosis without the need for random biopsies.

This research was conducted at the Massachusetts Institute of Technology Laser Biomedical Research Center and supported by the National Institute of Health (grants P41-RR02594 and R01-CA97966). C. Yu's e-mail address is chungyu@mit.edu.

*Current address, Department of Biomedical Engineering, University of Texas at Austin, Austin, Texas 78712.

†Also with the Department of Pathology, Harvard Medical School, Massachusetts General Hospital, Boston, Massachusetts 02114.

References

1. H. Fang, M. Ollera, E. Vitkin, L. M. Kimerer, P. B. Cipolloni, M. M. Zaman, S. D. Freedman, I. J. Bigio, I. Itzkan, E. B. Hanlon, and L. T. Perelman, IEEE J. Sel. Top. Quantum Electron. **9**, 267 (2003).
2. M. Bartlett, G. Huang, L. Larcom, and H. Jiang, Appl. Opt. **43**, 1296 (2004).
3. J. D. Wilson, C. E. Bigelow, D. J. Calkins, and T. H. Foster, Biophys. J. **88**, 2929 (2005).
4. J. D. Wilson and T. H. Foster, Opt. Lett. **30**, 2442 (2005).
5. L. Perelman, V. Backman, M. Wallace, G. Zonios, R. Manoharan, A. Nusrat, S. Shields, M. Seiler, C. Lima, T. Hamano, I. Itzkan, J. Van Dam, J. Crawford, and M. Feld, Phys. Rev. Lett. **80**, 627 (1998).
6. V. Backman, R. Gurjar, K. Badizadegan, I. Itzkan, R. Dasari, L. Perelman, and M. Feld, IEEE J. Sel. Top. Quantum Electron. **5**, 1019 (1999).
7. K. Sokolov, R. Drezek, K. Gossage, and R. Richards-Kortum, Opt. Express **5**, 302 (1999).
8. J. Mourant, J. Freyer, A. Hielscher, A. Eick, D. Shen, and T. Johnson, Appl. Opt. **37**, 3586 (1998).
9. H. C. van de Hulst, *Light Scattering by Small Particles* (Dover, New York, 1981).